Available online at www.sciencedirect.com
SCIENCE DIRECT®
Journal of Chromatography A, 1044 (2004) 277–285
JOURNAL OF CHROMATOGRAPHY A
www.elsevier.com/locate/chroma

On-chip electrochromatography using sol–gel immobilized stationary phase with UV absorbance detection

Rohit Jindal, Steven M. Cramer*

Howard P. Isermann Department of Chemical and Biological Engineering, Rensselaer Polytechnic Institute, Troy, NY 12180, USA

Abstract

A chromatography column on a chip was fabricated by immobilizing reversed-phase stationary phase particles (5 μm, C_4) using sol–gel technology. Channels were fabricated in quartz using photolithography and wet etching. Localization of the stationary phase was achieved by immobilizing the stationary phase at the desired location in the separation channel prior to bonding of the cover plate. Cross channel design was employed for gated injection. An optical fiber setup was developed for carrying out on-chip UV absorbance detection. The effective optical path length was theoretically determined for the trapezoidal shaped channel and the result was shown to match closely with the experimentally determined value. The effect of applied voltage on velocity was evaluated using thiourea as an unretained marker. Separation performance of the stationary phase was demonstrated by separation of three peptides (Trp–Ala, Leu–Trp and Trp–Trp) under isocratic chromatographic conditions.

Keywords: Sol–gel; Stationary phases, electrochromatography; Chip technology; Microfluidics; Detection, electrochromatography; Instrumentation; Peptides

1. Introduction

Microfluidic devices, also known as “lab-on-chip”, offer a number of advantages such as small sample requirements, fast analysis time and the ability to integrate several analytical steps (e.g. reaction, injection, separation and detection) on a single device. In recent years many reports have been published demonstrating the use of these devices for a variety of applications including cell analysis [1], clinical diagnostics [2–4], polymerase chain reaction [5], DNA sequencing and separation [6], chemical [7] and enzymatic [8] reactions, protein digestion and separation [9], and forensic analysis [10].

Since the conception of chip-based chemical analysis systems electrophoresis [11–13] has been the most widely used separation method on planar devices. A significant increase in the application of these devices could be achieved by incorporating chromatography as a separation technique. The main challenge in integrating chromatography is the difficulty associated with packing stationary phases into micrometer scale channels. In order to avoid packing, initial work involved modifying channel walls with functional groups [14] that acted as the stationary phase. While the surface modification approach demonstrated that chromatography can be carried out in a chip format, it suffers from low surface area to volume ratio resulting in lower capacities. According to the analysis done by Knox [15], mobile phase mass transfer becomes limiting if channel dimensions are >2 μm for open tubular devices. To overcome these limitations Regnier and coworkers [16,17] developed “collocated monolith support structures” (COMOSS) where they micromanufactured stationary phase supports directly in the channel. An additional modification step is then required for derivatizing the supports with functional groups. Micelle electrokinetic chromatography [18–20] was demonstrated using sodium dodecyl sulfate above its critical micelle concentration, however, it suffers from limited peak capacity. Another approach that is being pursued is the use of monolithic stationary phases [21,22] in which the stationary phase is formed by in situ polymerization of monomers in the channel. Monolithic stationary phases have been recently demonstrated on-chip-based devices for separation [23,24] and solid-phase extraction [25]. However, the range of functional groups that are currently available for carrying out chromatography in monoliths is not as wide as for particulate stationary phases.

It would be desirable to develop chromatographic chip systems with channels packed with stationary phase parti-

* Corresponding author. Tel.: +1 518 276 6198; fax: +1 518 276 4030.
E-mail address: crames@rpi.edu (S.M. Cramer).

0021-9673/$ – see front matter © 2004 Elsevier B.V. All rights reserved.
doi:10.1016/j.chroma.2004.05.065

cles, since these materials are well characterized and are readily available for carrying out different modes of chromatography. The most common method for packing stationary phase particles inside silica capillaries is to use a frit to hold the particles in place. There are a number of problems associated with using frits in these systems such as bubble formation, their unpredictable influence on electroosmotic flow and the difficulty associated with making frits in microfluidic devices. Ocvirk et al. [26] demonstrated the use of frits for packing the stationary phase particles in microchannels but poor separation was achieved using this system. Other approaches such as the tapered channel approach [27] and using a physical barrier [28] for packing of the particles have been demonstrated, but their use complicates the chip fabrication process.

Sol–gel technology offers an alternative for packing particles without using any frits. Sol–gels have recently become increasingly popular as an immobilization matrix for a variety of materials ranging from biological species like enzymes [29], cells [30] and antibodies [31] to chromatographic stationary phase material [32–35]. For chromatographic material immobilization two approaches have been employed: (i) packing the capillary with stationary phase particles in the presence of a frit and subsequently filling the capillary with sol–gel to hold the particles together after removal of the frit. (ii) Introducing the suspension of stationary phase particles in the sol–gel precursor solution into the capillary and allowing it to gel. Sol–gels have also been used for preparing freely standing structures on solid substrate where patterning is achieved using the micromolding in capillaries (MIMIC) technique. This technique has been used for preparing optical waveguides [36], photonic laser crystals [37] and patterned nanostructured films [38].

In the present report, channels are fabricated in quartz. Stationary phase is then formed at a desired location within the separation channel by immobilizing reversed phase stationary phase particles in the sol–gel and subsequently the cover plate is bonded to close the channel. Using this technique, stationary phase can be packed without complicating the chip fabrication process.

2. Experimental

2.1. Chemicals and reagents

Tryptophan–alanine (Trp–Ala), diethyleneglycolmonoethyl ether (DEME), leucine–tryptophan (Leu–Trp), trytophan–tryptophan (Trp–Trp), thiourea and [2-(*N*-Morpholino) ethanesulfonic acid] (MES) were purchased from Sigma (St. Louis, MO, USA). Poly(vinyl acetate) (PVAc; MW = 167,000), toluene, isopropanol, hydrochloric acid (0.964 M) and tetraethylorthosilicate (TEOS) were obtained from Aldrich (Milwaukee, WI, USA). Naphthalene was purchased from Supelco (Bellefonte, CA, USA). Acetonitrile (ACN), sodium hydroxide, acetone, methanol and ethanol were purchased from Fisher Scientific (Fairlawn, NJ, USA). Nitric acid and hydrofluoric acid were purchased from J.T. Baker (Phillipsburg, NJ, USA). Poly(dimethylsiloxane) (PDMS) (Sylgard184 silicone elastomer, Midland, MI, USA) was obtained from Ellsworth Adhesives (Germantown, WI, USA).

Stationary phase particles (C_4 modified silica, 5 μm, 300 Å pore size, Vydac, Hesperia, CA, USA) were suspended in acetonitrile and centrifuged. The supernatant was discarded and the particles were dried using a hot plate until particles were obtained in the form of free flowing powder.

2.2. Chip fabrication

Channels were fabricated in a quartz (3 in. × 3 in. × 1/16 in.; 1 in. = 2.54 cm; G.M. Associates, Oakland, CA, USA) slide using photolithography and wet etching. The photo mask for patterning was designed using corel draw and printed out on a transparency using a high-resolution printer (Atlantic Digital Images, Latham, NY, USA). Transparency masks provide a cheap and quick alternative to chrome mask. Quartz slides were cleaned with acetone, isopropanol and deionized water. The 250 Å thick chromium and 1000 Å thick gold (International Advanced Materials, Spring Valley, NYM, USA) were deposited sequentially on quartz using e-beam evaporation. Chromium improves the adhesion of gold to quartz. Gold acts as the hard mask during etching. Hexamethyldisilanzane (HMDS) (Microprime Primer P-20; Shin Etsu Microsi, Phoenix, AZ, USA) was spin coated on gold at 3000 rpm for 25 s. This was followed with spin coating of the positive photoresist, S1813 (Shipley, Marlborough, MA, USA), at 3000 rpm for 40 s. The sample was then baked at 100 °C for 1 min. The channel pattern was photolithographically transferred to resist using a contact mask aligner (MJB3, Karl Suss, Waterbury Center, VT, USA). After 2 min development in AZ 300 MIF developer solution (Clariant, Somerville, NJ, USA) resist was hard baked at 120 °C for 30 min. Exposed gold was etched using gold etching solution (Transene company, Rowley, MA, USA) for 2 min. Chromium etching solution etched the chromium in 1 min and exposed the quartz. Finally, a mixture of HF–HNO_3 (210:95) solution was used for etching the quartz. A depth of 43 μm was obtained in 50 min. Access holes were drilled in quartz using diamond tipped drill and these holes acted as sample (S), buffer (B), sample waste (SW) and waste (W) reservoirs. Design of the channels used in this work is standard cross channel design as shown in Fig. 1.

PDMS slabs were prepared by mixing pre-polymer solution with the curing agent in a ratio of 10:1. The mixture was degassed for 1 h and then poured in a petri-dish, which was subsequently heated at 60 °C for 2 h. PDMS slabs of desired dimensions were then sectioned using a knife.

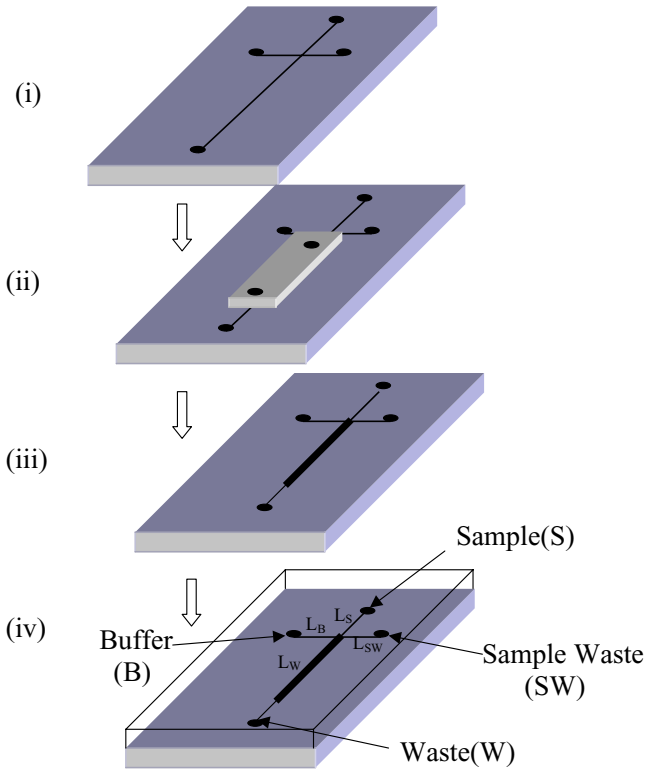

Fig. 1. Schematic for the process of immobilization of the stationary phase in the channel. (i) Microfabricated quartz chip with cross channel design. (ii) PDMS slab bonded reversibly to the quartz, defining the location of the stationary phase. (iii) Quartz with stationary phase particles immobilized in the separation channel after removing the PDMS cover. (iv) Bonding of PDMS and quartz after oxygen plasma treatment. $L_B = 1.2$ cm, $L_S = 0.8$ cm, $L_{SW} = 1.2$ cm, $L_W = 4.6$ cm.

2.3. Stationary phase formation

Stationary phase was formed in the channel prior to bonding of the cover plate in contrast to most reports published in the literature. Stationary phase particles were immobilized in the sol–gel using a slight modification of the method developed by Dulay et al. [32]. Sol–gel solution was prepared by mixing TEOS (20 μl), HCl (0.12 M, 10 μl) and DEME (70 μl). C_4 silica particles were added to the above solution to give a final concentration of 250 mg/ml. The suspension was allowed to stand for 5 h and was then agitated using a vortex mixer before introducing it into the channel.

The quartz slide with micro channels was spin coated with PVAc–toluene (5%, w/v) solution at 3000 rpm for 40 s. PDMS surface was silanized with (tridecafluoro-1,1,2,2-tetrahydrooctyl)-1-trichlorosilane (United Chemical Technologies, Bristol, PA, USA) using a vacuum desicator. Silanized PDMS was brought in contact with PVAc coated quartz slide and formed a reversible seal with quartz. Spatial control over the stationary phase was achieved by selectively filling the suspension of particles in the desired part of the separation channel using PDMS as shown in Fig. 1. As seen in figure, the PDMS used during column formation had openings at the two ends of the column segment to enable proper priming with the stationary phase suspension. The particle suspension was introduced into the separation channel in the following manner. As the suspension of particles was introduced at one end of the separation channel with a pipette, it filled part of the channel by capillary action. To achieve complete filling of the desired part of the channel, a vacuum was applied at the other end using a peristaltic pump (Millipore, 6–600 rpm) operating at 50 rpm. The suspension was allowed to gel at room temperature for 5 h. Once the suspension turned opaque, the PDMS slab was peeled off from the quartz slide leaving the sol–gel immobilized stationary phase in the channel. The chip was kept in an oven and temperature of the oven was increased to 120 °C at a rate of 1 °C/min. Temperature of the oven was maintained at 120 °C for 24 h. The chip was removed from the oven once the temperature dropped down to room temperature. The quartz chip, with stationary phase, and a fresh PDMS slab were cleaned with methanol and bonded irreversibly after oxygen plasma treatment to hydrophilize the PDMS. Chips were stored in the buffer solution immediately after bonding to maintain the hydrophilic nature of PDMS.

2.4. Absorbance detection

On-chip UV absorbance detection of samples was carried out using an in house built experimental setup. The chromatographic chip was placed on an XYZ translation stage and the chip was positioned between two optical fibers (P-600-2-SR, Ocean Optics, Dunedin, FL, USA) as shown in Fig. 2a so that the channel was aligned between the fibers. The top optical fiber was connected to a deuterium–tungsten light source (DT-1000-REM-MD, Ocean Optics) and provided the incident light. There was a lens at the outlet of the light source that focused the light into the top optical fiber. The bottom optical fiber collected the transmitted light and carried it to the CCD array detector (S2000, Ocean Optics) that was equipped with a 200 μm entrance slit and a lens that collected the light from the bottom optical fiber. Data were collected using the software OOIBase32 (Ocean Optics).

2.5. Voltage control and chip operation

Voltage control on the chip was achieved using two 0–3 KV high voltage power supplies (Bertan Associates, Syosett, NY, USA) and (Power Designs, Westbury, NY, USA). Platinum wires (Alfa Aesar, Ward Hill, MA, USA) were placed in the reservoirs and provided the electrical contact between chip and power supplies. Buffer and sample reservoirs were connected to two power supplies, which provided independent voltages. A potentiometer (CU5052, Ohmite, Skokia, IL, USA) was connected to one of the power supplies and provided reduced voltage in sample waste reservoir. A high-voltage reed relay (Ross Engineer-

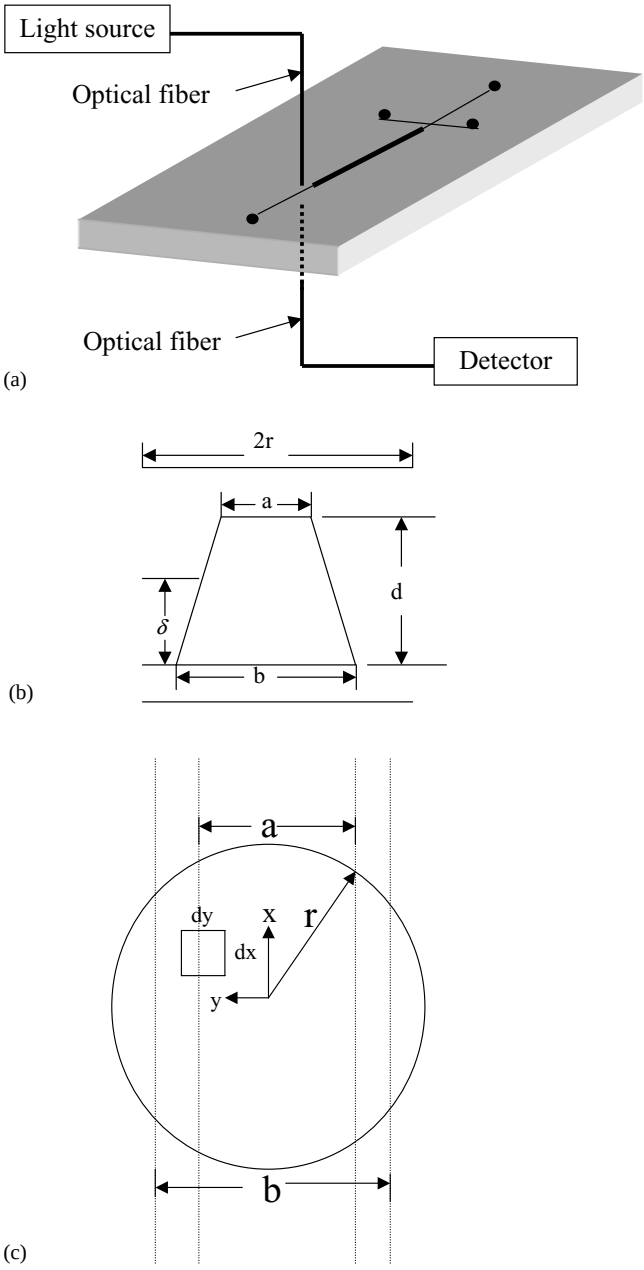

Fig. 2. (a) Schematic of the optical fiber setup for UV absorbance detection on the chip. (b) Cross section of the channel; 2*r*, diameter of optical fiber; *a*, channel width at the top of the channel; *b*, channel width at the bottom of channel; *d*, depth of the channel; *δ*, path length experienced by the light. (c) Top view of the optical fiber setup. (*Note*: figures are not drawn to scale).

ing, Campbell, CA, USA) was employed for floating the voltage in the buffer reservoir.

Chips were conditioned for 2 h with the mobile phase before starting the chromatographic experiments. The mobile phase used for the analysis was MES (20 mM, pH 6) buffer–acetonitrile (95:5, (v/v)). The mobile phase was degassed for 20 min using helium before introducing it in the reservoirs.

2.6. Scanning Electron Microscopy (SEM) Analysis

Samples were prepared by sectioning a small part of the chip with sol–gel before bonding of the PDMS. Samples were made conducting by sputtering platinum. Scanning electron micrographs were obtained at an applied voltage of 10 KeV using SEM (JEOL JSM-840).

3. Results and discussion

3.1. Stationary phase

After microfabrication of the chip was carried out, the separation channel was filled with the stationary phase using the sol–gel approach. Localization of stationary phase was achieved by selectively filling the desired part of the separation channel. A PDMS slab of desired dimension provided the cover for selective filling as shown in Fig. 1. As suspension of particles was introduced from one end, it filled part of the channel by capillary action. To achieve complete filling of the desired part of the channel, a vacuum was applied at the other end using a peristaltic pump. After the desired region of the channel was primed, the solution was allowed to gel. Fig. 3a and b show that the stationary phase was present only in the desired part of the separation channel while the injection cross (Fig. 3a) and detection part (Fig. 3b) of the channel were free of stationary phase. Once gelation was complete, the PDMS was peeled off. Obviously, it is critical that the stationary phase remains attached to the quartz as the PDMS is removed. To achieve this goal, surface modification of both PDMS and quartz was carried out before introduction of the stationary phase. Quartz was spin coated with PVAc to enhance its adhesion to the sol–gel [31]. Silanization of the PDMS surface [36] prior to bonding to the quartz enabled removal of the PDMS without dislodging sol–gel from the channel.

In our approach, the stationary phase was packed before bonding of the cover plate. Thus, it is critical that the sol–gel processing not result in any shrinkage of the resulting sol–gel stationary phase composite. Initial attempts to fabricate the chromatography chip employed similar conditions as described by Dulay et al. for capillary systems [32]. When ethanol was employed as the solvent in the sol–gel mixture, the resulting column exhibited large gaps that were created after gelation of the sol in the channel. Sol–gel is known to shrink and crack during the heating step, however, in the presence of particles cracking and shrinkage of sol–gel is minimized [32,33,39]. Under the ethanol solvent conditions, the results indicate that the presence of the particles was not sufficient for eliminating the shrinkage. In an attempt to eliminate the gaps, ethanol was replaced with DEME as the solvent in the sol–gel precursor mixture. As shown in Fig. 4 this process resulted in the entire cross section of the channel being filled with stationary phase particles held together by the sol–gel with minimal shrinkage. It is believed that in the

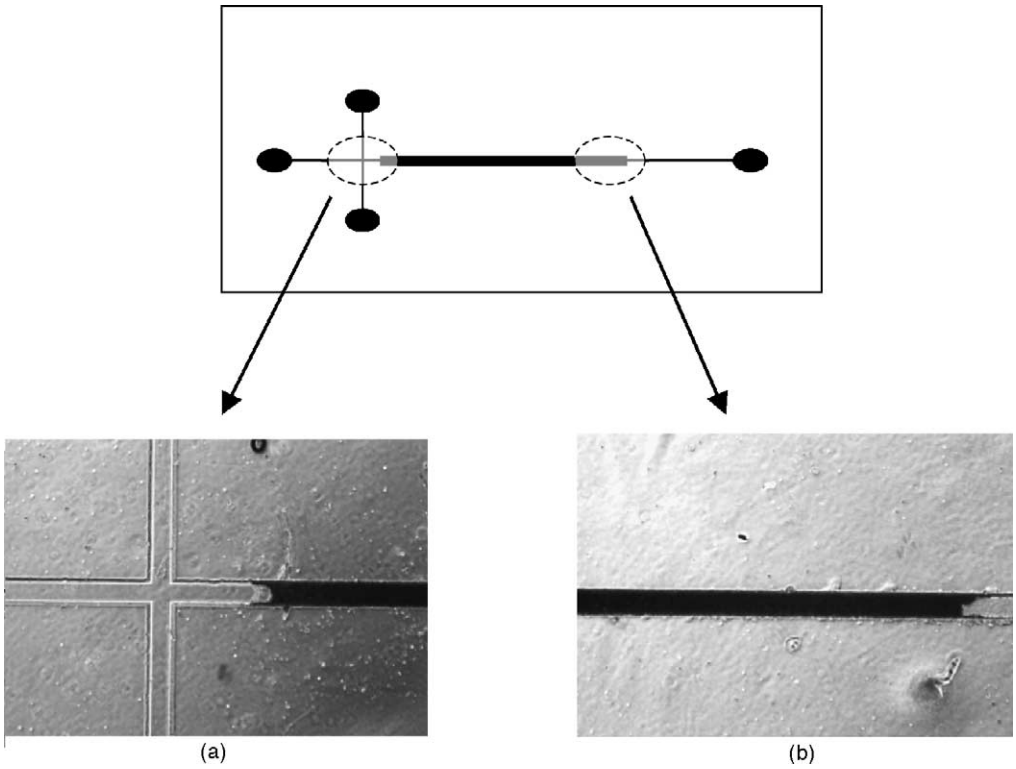

Fig. 3. Optical micrographs showing localization of the stationary phase. (a) Cross channel design with injection channels free from stationary phase. (b) Part of separation channel from detection side with stationary phase ending before detection point.

presence of the particles, stress that is produced due to the capillary pressure during drying is relaxed due to the strong bonding between particles and the sol–gel. Capillary stresses might be reduced due to the higher boiling point of DEME resulting in lower evaporation rates as compared to ethanol with a reduction in the shrinkage of the sol–gel. While no gaps were observed in the separation channel in the presence of DEME, the gelation time was increased as compared to ethanol. Higher viscosity of DEME as compared to ethanol might be responsible for the increased gelation time.

3.2. Absorbance detection

An optical fiber setup was employed as described in the experimental section to carry out on-chip UV absorbance detection. In order to evaluate the linearity of the detector, a step input of thiourea was made by applying a voltage of 500 V across reservoir (B) and (SW) (Fig. 1b). The detection point was located 1 cm from reservoir (B). The concentration of thiourea was varied from 125 μM to 4 mM. The detector response can be described by the equation.

$$y = 0.026x \quad (1)$$

with $R^2 = 0.99$, where y is the absorbance, x the concentration (mM) of thiourea and R^2 is the regression coefficient. The limit of detection (LOD) was estimated from the value at which signal/noise (S/N) was equal to 2. The noise at 240 nm was estimated to be 2 mA U, which gave a LOD of 167 μM for thiourea. The LOD can be improved by decreasing the noise. The main source of noise is the fluctuation in the output of the deuterium light source. Incorporation of a bifurcated optical fiber and a second detector would allow reference monitoring as used in standard spectrometers employed for absorbance detection, resulting in an improved LOD.

The dimensions of the trapezoidal channel as measured with a profilometer were: 350 μm width at the top and 150 μm at the bottom with a depth of 43 μm. To calculate the effective path length (L_{eff}), the extinction coefficient (ε) of thiourea was determined using a spectrometer equipped with a standard 1 cm path length cuvette. The effective path length was calculated using the Lambert–Beer law:

$$A = \varepsilon c L_{eff} \quad (2)$$

where A is the absorbance and C the concentration of the analyte. (A/C) was estimated from the slope of Eq. (1). L_{eff} was calculated to be 23 μm, which is 53% of the depth of channel. In order to explain the discrepancy between L_{eff} and the depth of the channel, L_{eff} was estimated theoretically, taking into account the trapezoidal geometry of the channel and stray light passing through the chip as described below.

Transmission of light through the channel can be calculated in a similar fashion to that described by Hjertén [40] for a cylindrical cell. The assumptions made while formulating the expression for the transmission coefficient (T) in Eq. (3) are: reflection and refraction of light is neglected;

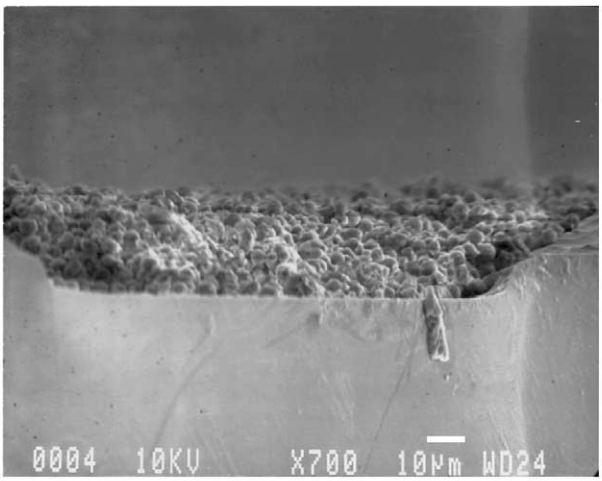

(a)

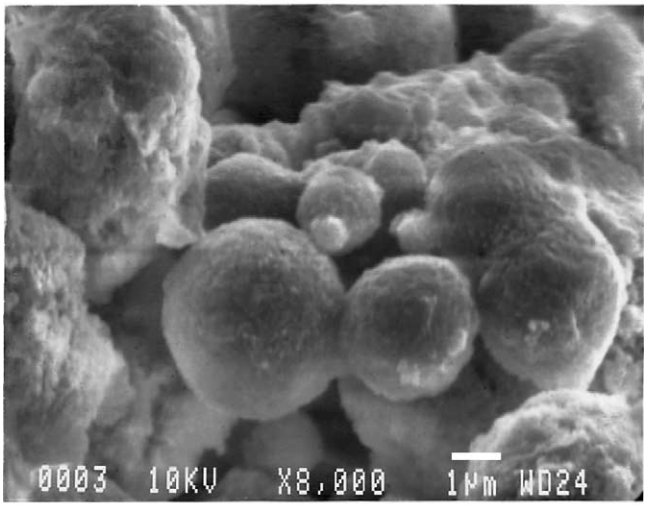

(b)

Fig. 4. Scanning electron micrographs of the stationary phase. (a) Complete channel cross section filled with the stationary phase. (b) Section at higher magnification showing particles held together with sol–gel.

light coming out of the optical fiber is uniform; all the transmitted light is collected by the bottom optical fiber; and divergence of light as it travels down from the top to bottom optical fiber can be neglected.

$$T = \frac{z}{z_0} = \frac{\int_0^r \int_0^{\sqrt{r^2-x^2}} e^{-(\ln(10)\varepsilon C\delta(x,y))}\,\mathrm{d}y\,\mathrm{d}x}{(\pi/4)r^2} \tag{3}$$

where z is the number of photons that pass through the chip in the presence of analyte that shows absorbance, z_0 the number of photons in the absence of absorbance, r the radius of the optical fiber, δ the path length, and x and y are as shown in Fig. 2c.

For low values of absorbance (A $<$ 0.1), T can be simplified [41] and an analytical expression for L_{eff} can be derived by expanding the exponential term in the Eq. (3) while ignoring the higher order terms.

$$T \approx \frac{\int_0^r \int_0^{\sqrt{r^2-x^2}} \mathrm{d}x\,\mathrm{d}y - \int_0^r \int_0^{\sqrt{r^2-x^2}} \ln(10)\varepsilon C\delta(x,y)\,\mathrm{d}x\,\mathrm{d}y}{(\pi/4)r^2} \tag{4}$$

$$T = 1 - \frac{\ln(10)\varepsilon C \int_0^r \int_0^{\sqrt{r^2-x^2}} \delta(x,y)\,\mathrm{d}x\,\mathrm{d}y}{(\pi/4)r^2} \tag{5}$$

$$T \approx \exp\left\{-\ln(10)\varepsilon C\left[\frac{\int_0^r \int_0^{\sqrt{r^2-x^2}} \delta(x,y)\,\mathrm{d}x\,\mathrm{d}y}{(\pi/4)r^2}\right]\right\} \tag{6}$$

$$A = -\log(T) = \varepsilon C\left(\frac{\int_0^r \int_0^{\sqrt{r^2-x^2}} \delta(x,y)\,\mathrm{d}x\,\mathrm{d}y}{(\pi/4)r^2}\right) \tag{7}$$

On comparing Eqs. (7) and (2):

$$L_{\mathrm{eff}} = \left(\frac{\int_0^r \int_0^{\sqrt{r^2-x^2}} \delta(x,y)\,\mathrm{d}x\,\mathrm{d}y}{(\pi/4)r^2}\right) \tag{8}$$

$\delta(x, y)$ is given by the following expression.

$$\delta(x,y) = \begin{cases} d; & 0 < y < \dfrac{a}{2}; & 0 < x < rB \\ \dfrac{(b/2)-y}{(b-a)/2}d; & \dfrac{a}{2} < y < \dfrac{b}{2}; & 0 < x < rB \\ 0; & \dfrac{b}{2} < y < \sqrt{r^2-x^2}; & 0 < x < rB \\ d; & 0 < y < \dfrac{a}{2}; & rB < x < rA \\ \dfrac{(b/2)-y}{(b-a)/2}d; & \dfrac{a}{2} < y < \sqrt{r^2-x^2}; & rB < x < rA \\ d; & 0 < y < \sqrt{r^2-x^2}; & rA < x < r \end{cases}$$

where a, b and d are defined in Fig. 2b and c;

$$B = \sqrt{1-\left(\frac{b^2}{4r^2}\right)}; \qquad A = \sqrt{1-\left(\frac{a^2}{4r^2}\right)}$$

Eq. (8) was solved analytically by substituting $\delta(x, y)$ to obtain:

$$\frac{L_{\mathrm{eff}}}{d} = 1 - \frac{2}{\pi(b-a)}\left\{b\sin^{-1}(B) - a\sin^{-1}(A) + 2r(B-A)\left[\frac{1}{3}(A^2+B^2+AB)-1\right]\right\} \tag{9}$$

Upon substituting values of a (150 μm), b (350 μm) and r (300 μm) in Eq. (9) L_{eff}/d is equal to 0.51 which is in very close agreement with the value of 0.53 obtained from experiments.

3.3. Partitioning in PDMS

While the channels were fabricated in quartz, the cover for the channel was made of PDMS. Initial experiments on the separation of polycyclic aromatic hydrocarbons (PAHs) resulted in no signal at the detection point due to partitioning of the analytes into the PDMS cover. There have been

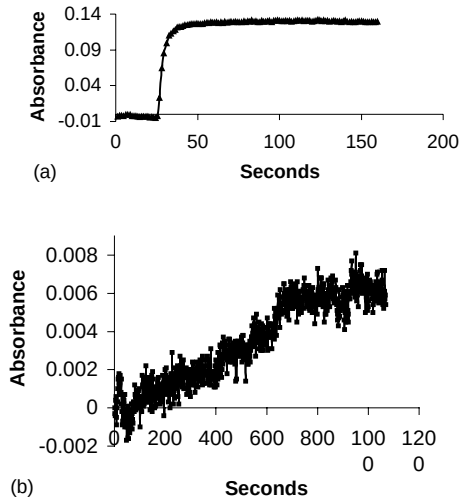

Fig. 5. Evaluation of partitioning in PDMS. (a) Step input of thiourea in an empty channel with the following voltages applied to the reservoirs: buffer reservoir = 600 V, and sample waste reservoir = 0 V. The detection point was located at 8 mm from the buffer reservoir, i.e. 2/3 of the way towards the cross. Wavelength = 240 nm; mobile phase: 20 mM MES (pH 6)–ACN (95:5 (v/v)). (b) Step input of naphthalene under the same conditions as in (a).

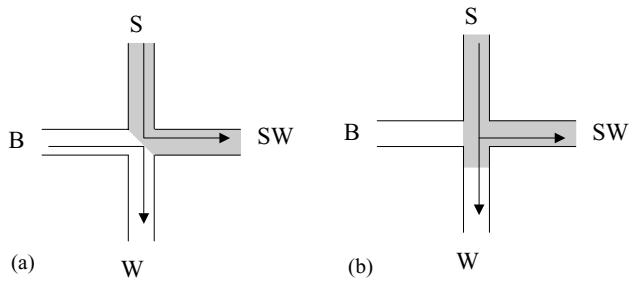

Fig. 6. Schematic of injection of samples using gated injection method. (a) Separation mode; applied voltage ratio (*B*/*S*/SW/*W*: 1.2/1/0.55/0. *Note*: See Fig. 1 for definition of reservoirs). (b) Injection mode; applied voltage ratio (*S*/SW/*W*: 1/0.55/0) with buffer reservoir (*B*) floated for the injection.

numerous reports in the literature about the partitioning of hydrophobic molecules in PDMS [17,27,42]. Partitioning in PDMS was evaluated by carrying out breakthrough experiments in an empty channel. A step input of the analytes was made by applying 600 V to reservoir (B), while reservoir (SW) was grounded. As shown in Fig. 5a, the outlet profile for thiourea exhibits a sharp breakthrough which is expected, since it does not partition into PDMS.

In contrast, the breakthrough front for naphthalene under the same conditions deviates significantly from the step profile as shown in Fig. 5b.These breakthrough experiments can be readily employed as an initial screen to test the partitioning of analytes into the PDMS.

3.4. Velocity studies

Electroosmotic flow velocity was calculated using thiourea as an unretained marker. Pulse injection of thiourea was made using the gated injection [43] method as shown in Fig. 6. Voltages were applied to the sample (*S*), buffer (*B*), sample waste (SW) and waste (*W*) reservoirs in the ratio of 1:1.2:0.55:0, respectively. The sample was injected by floating the buffer reservoir for 5 s. The gated injection method was used since it provides the flexibility of injecting larger sample volumes, which is required due to the relatively low sensitivity of the on-chip UV absorbance detection due to the short path length. Detection was carried out at a distance of 26 mm from the cross in the separation channel (Fig. 2a). The sample reservoir voltage was varied from 500 to 2500 V to change the flow velocity while keeping the voltages of the reservoirs in the ratios given above. The electric field was calculated by dividing the potential at the cross by the total length from the cross to the waste reservoir. Initially resistance of different channels was calculated by measuring the current in the channels upon application of voltages in the reservoirs.

Voltage at the cross was calculated using Kirchoff's law. As expected, velocity followed the electric field linearly [44] and can be described by the equation:

$$y = 0.0014x \tag{10}$$

with $R^2 = 0.99$, where y is the velocity (mm/s), x the electric field (V/cm). This implies that any nonlinear effects like Joule heating are absent for the applied field range. The use of a zwitterionic buffer MES as the mobile phase also aided in reducing the current and the Joule heating.

The efficiency of the peaks was calculated using standard expressions for the plate height and theoretical number of plates.

$$H = \frac{L}{N} \tag{11}$$

$$N = 5.54\left(\frac{t_r}{t_{w1/2}}\right)^{1/2} \tag{12}$$

where H is the plate height, L the length of the packed segment, N the number of plates, t_r the retention time and $t_{w1/2}$ the width of the peak at half height. The efficiency obtained for the unretained thiourea was approximately 30 μm and was found to be relatively independent with velocity for the ranges studied. Two prototypes of this chip system were assembled and comparable results were obtained with both systems. Clearly, the efficiency of thiourea is much lower then that obtained using standard capillaries packed with particles. There are number of factors that could be responsible for this relatively low efficiency. Sol–gel synthesis was carried out under acidic conditions where it is known that micropores can form in sol–gel [45]. This can result in double layer overlap in the micropores, which would change the flow profile from plug to parabolic. Another factor to consider is the hybrid nature of the chip. Three walls of the channel (quartz) have the same ς potential while

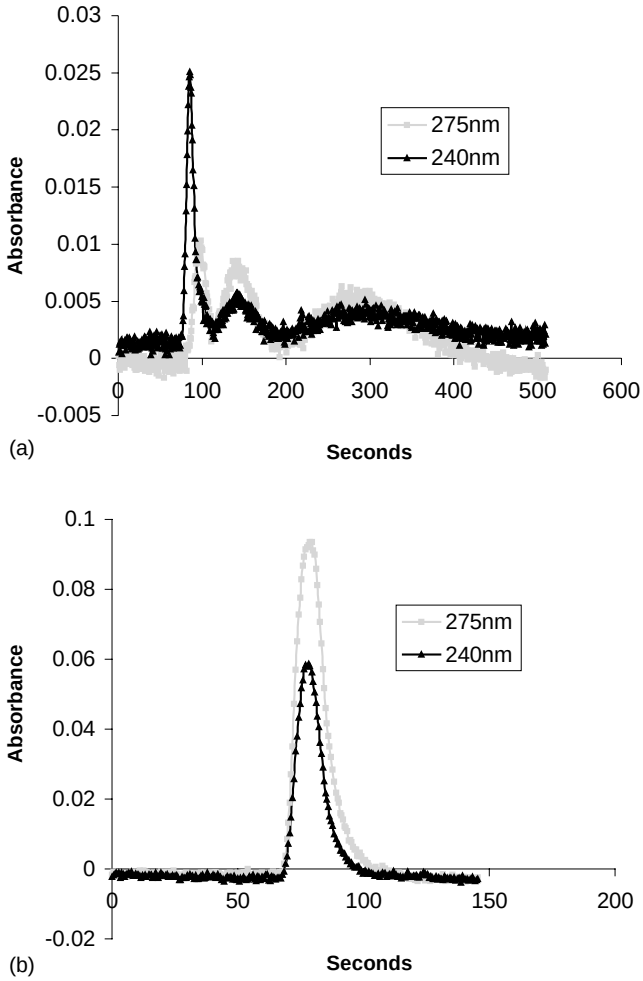

Fig. 7. Electrochromatogram obtained upon injection of a mixture of thiourea and the peptides: Trp–Ala, Leu–Trp, and Trp–Trp. Detection was carried out at two wavelengths: 240 and 275 nm. (a) Separation of peptides and thiourea using C_4 modified silica particles (5 μm, 300 Å pore size) immobilized in the sol–gel. (b) Co-elution of the peptides and thiourea in a chip prepared without any stationary phase. (*Note*: Mobile phase conditions were the same as in Fig. 5).

the cover (PDMS) has a different ς potential. This may lead to higher dispersion as compared to channels made up of a single material [46]. Ideas for improving the efficiency of this approach are described in the conclusions section.

3.5. Separation of peptides

In orer to demonstrate that this chromatographic chip system can be employed for separations, a four component separation was carried out. The feed mixture consisted of thiourea (unretained marker) and the peptides Trp–Ala, Leu–Trp and Trp–Trp. Mobile phase conditions were selected (e.g. pH 6.0) so that the three peptides had no net charge in order to minimize the effect of electrophoretic migration. As shown in Fig. 7a, the three peptides were separated in the order of their hydrophobicity with Trp–Ala coming out first, followed by Leu–Trp and Trp–Trp. As seen in figure, the peptides were well resolved using this isocratic separation in the short 2.5 cm chip column. The on-chip UV absorbance detection system used in this work enables the simultaneous monitoring of several wavelengths. In this experiment, the absorbance signal was recorded at two different wavelengths, 240 and 275 nm. At 275 nm, thiourea has negligible absorbance, thus even though thiourea and Trp–Ala were not resolved under these conditions, it is possible to identify the peaks corresponding to the two analytes by looking at the two wavelengths simultaneously. In order to confirm that this peptide separation was due to chromatography rather than electrophoresis, the mixture of peptides and thiourea was injected in the chip without any stationary phase. As shown in Fig. 7b all the analytes co-eluted in the absence of stationary phase. The results shown in Fig. 7 demonstrate that separations can indeed be carried out in chromatographic chip systems using sol–gel immobilized stationary phase materials. Future work will focus on improving the performance of this chromatographic chip system as described below.

4. Conclusions

Packing of stationary phase particles using sol–gel technology has been successfully demonstrated on a chip system. A simple procedure has been developed that allows both immobilization and localization of the stationary phase in the desired part of the channel. This approach offers complete freedom in terms of the design of the microchip as no additional channels for the introduction of the beads are required. In addition all the channels can be of equal width and depth that considerably simplifies the chip fabrication process. A simple optical fiber setup has been developed for carrying out multi-wavelength UV absorbance detection on the chip.

In this paper preliminary results are presented that demonstrate that separations can indeed be carried out in chromatographic chip systems using sol–gel immobilized stationary phase materials. However, the performance of this system must be improved in the future in order to carry out more complicated separations. Future work will examine several approaches for improving this technology. In the present system, three walls of the channel (quartz) have the same ς potential while the cover (PDMS) has a different ς potential. This may lead to higher dispersion as compared to the channels made of single material [46]. This issue will be resolved in the future by carrying out low temperature bonding of the quartz using HF [47] or sodium silicate [48] bonding. Alternatively, we will examine the utility of chips completely made out of PDMS. We will also examine the effect of using smaller particle diameter stationary phase materials as well as optimizing sol–gel synthesis conditions. Finally, gradient operation will be examined to significantly broaden the utility of this chip-based system.

Acknowledgements

The authors acknowledge Professor Joel Plawsky at Rensselaer for useful discussions about sol–gel techniques and for allowing us to use his facilities. We would also like to thank Professor Mark Burns at the University of Michigan for allowing RJ to visit his laboratory in the early part of this work. Clean room support for this work was provided by Rensselaer.

References

[1] A.Y. Fu, C. Spence, A. Scherer, F.H. Arnold, S.R. Quake, Nat. Biotechnol. 19 (1999) 1109.
[2] K. Sato, M. Tokeshi, H. Kimura, T. Kitamori, Anal. Chem. 73 (2001) 1213.
[3] N.J. Munro, Z.L. Huang, D.N. Finegold, J.P. Landers, Anal. Chem. 72 (2000) 2765.
[4] N. Chiem, D. Harrison, Anal. Chem. 69 (1997) 373.
[5] J. Khandurina, T.E. McKnight, S.C. Jacobson, L.C. Waters, R.S. Foote, J.M. Ramsey, Anal. Chem. 72 (2000) 2995.
[6] S.R. Liu, H.J. Ren, Q.F. Gao, D.J. Roach, R.T. Loder, T.M. Armstrong, Q.L. Mao, I. Blaga, D.L. Barker, S.B. Jovanovich, Proc. Natl. Acad. Sci. U.S.A. 97 (2000) 5369.
[7] M.C. Mitchell, V. Spikmans, A.J. de Mello, Analyst 126 (2001) 24.
[8] J. Wang, M.P. Chatrathi, B.M. Tian, R. Polsky, Anal. Chem. 72 (2000) 2514.
[9] N. Gottschlich, C.T. Culbertson, T.E. McKnight, S.C. Jacobson, J.M. Ramsey, J. Chromatogr. B 745 (2000) 243.
[10] S.R. Wallenborg, I.S. Lurie, D.W. Arnold, C.G. Bailey, Electrophoresis 21 (2000) 3257.
[11] D.C. Duffy, J.C. McDonald, O.J.A. Schueller, G. Whitesides, Anal. Chem. 70 (1998) 4974.
[12] S.C. Jacobson, C.T. Culbertson, J.E. Daler, J.M. Ramsey, Anal. Chem. 70 (1998) 3476.
[13] Y.N. Shi, P.C. Simpson, J.R. Scherer, D. Wexler, C. Skibola, M.T. Smith, R.A. Mathies, Anal. Chem. 71 (1999) 5354.
[14] S.C. Jacobson, R. Hergenröder, L.B. Koutny, J.M. Ramsey, Anal Chem. 66 (1994) 2369.
[15] J.H. Knox, J. Chromatogr. Sci. 18 (1980) 453.
[16] B. He, N. Tait, F.E. Regnier, Anal. Chem. 70 (1998) 3790.
[17] B.E. Slentz, N.A. Penner, E. Lugowska, F. Regnier, Electrophoresis 22 (2001) 3736.
[18] A.W. Moore, S.C. Jacobson, J.M. Ramsey, Anal. Chem. 67 (1995) 4184.
[19] J.P. Kutter, S.C. Jacobson, J.M. Ramsey, Anal. Chem. 69 (1997) 5165.
[20] F. von Heeren, E. Verpoorte, A. Manz, W. Thormann, Anal. Chem. 68 (1996) 2044.
[21] E.C. Peters, M. Petro, F. Svec, J.M.J. Frechet, Anal. Chem. 69 (1997) 3646.
[22] C. Yu, F. Svec, J.M.J. Frechet, Electrophoresis 21 (2000) 120.
[23] C. Ericson, J. Holm, T. Ericson, S. Hjertén, Anal. Chem. 72 (2000) 81.
[24] D.J. Throckmorton, T.J. Shepodd, A.K. Singh, Anal. Chem. 74 (2002) 784.
[25] C. Yu, M.H. Davey, F. Svec, J.M.J. Frechet, Anal. Chem. 73 (2001) 5088.
[26] G. Ocvirk, E. Verpoorte, A. Manz, M. Grasserbauer, H.M. Widmer, Anal. Methods Instrum. 2 (1995) 74.
[27] L. Ceriotti, N.F. de Rooij, E. Verpoorte, Anal. Chem. 74 (2002) 639.
[28] R.D. Oleschuk, L.L. Shultz-Lockyear, Y. Ning, D.J. Harrison, Anal. Chem. 72 (2000) 585.
[29] K. Sakai-Kato, M. Kato, T. Toyo'oka, Anal. Chem. 75 (2003) 388.
[30] A. Coiffier, T. Coradin, C. Roux, O.M.M. Bouvet, J. Livage, J. Mater. Chem. 11 (2001) 2039.
[31] Y.D. Kim, C.B. Park, D.S. Clark, Biotechnol. Bioeng. 73 (2001) 331.
[32] M.T. Dulay, R.P. Kulkarni, R.N. Zare, Anal. Chem. 70 (1998) 5103.
[33] Q.L. Tang, N.J. Wu, M.L. Lee, J. Microcol. Sep. 12 (2000) 6.
[34] G. Chirica, V.T. Remcho, Electrophoresis 20 (1999) 50.
[35] C.K. Ratnayake, C.S. Oh, M.P. Henry, J. Chromatogr. A 887 (2000) 277.
[36] C. Marzolin, S.P. Smith, M. Prentiss, G.M. Whitesides, Adv. Mater. 10 (1998) 571.
[37] O.J.A. Schuller, G.M. Whitesides, J. A Rogers, M. Meier, A. Dodabalapur, Appl. Opt. 38 (1999) 5799.
[38] M. Trau, N. Yao, E. Kim, Y. Xia, G.M. Whitesides, I.A. Aksay, Nature 390 (1997) 674.
[39] D.A. Barrow, T.E. Petroff, M. Sayer, Surf. Coat. Technol. 76 (1995) 113.
[40] S. Hjertén, Chromatogr. Rev. 9 (1967) 122.
[41] G.J.M. Bruin, G. Stegeman, A.C. Van Asten, X. Xu, J.C. Kraak, H. Poppe, J. Chromatogr. 559 (1991) 163.
[42] R. Muzzalupo, G.A. Ranieri, G. Golemme, E. Drioli, J. Appl. Polym. Sci. 74 (1999) 1119.
[43] S.C. Jacobson, S.V. Ermakov, J.M. Ramsey, Anal. Chem. 71 (1999) 3273.
[44] G. Choudhary, C. Horvath, J. Chromatogr. A 781 (1997) 161.
[45] C.J. Brinker, R.W. Scherer, Sol–Gel Science: The Physics and Chemistry of Sol–Gel Processing, Academic Press, New York, 1990.
[46] F. Bianchi, F. Wagner, P. Hoffmann, H.H. Girault, Anal. Chem. 73 (2001) 829.
[47] H. Nakanishi, T. Nishimoto, M. Kanai, T. Saitoh, R. Nakamura, T. Yoshida, S. Shoji, Sens. Actuators A 83 (2000) 136.
[48] H.Y. Wang, R.S. Foote, S.C. Jacobson, J.H. Schneibel, J.M. Ramsey, Sens. Actuators B 45 (1997) 199.